Article

Analysis of the Applicability of the Parabolic Trough Solar Thermal Power Plants in the Locations with a Temperate Climate

Tomasz Janusz Teleszewski [1,*], Mirosław Żukowski [1,*], Dorota Anna Krawczyk [1,*] and Antonio Rodero [2]

[1] Department of HVAC Engineering, Bialystok University of Technology, 15-351 Bialystok, Poland
[2] Grupo de Física de Plasma: Modelos, Diagnosis y Aplicaciones, Campus of Rabanales, Universidad de Córdoba, E-14071 Córdoba, Spain; fa1rosea@uco.es
[*] Correspondence: t.teleszewski@pb.edu.pl (T.J.T.); m.zukowski@pb.edu.pl (M.Z.); d.krawczyk@pb.edu.pl (D.A.K.); Tel.: +48-797-995-926 (D.A.K.)

Abstract: Currently, intensive work is underway in Poland to increase the share of renewable energy sources in the overall energy balance. Therefore, this paper presents the possibilities of using concentrated solar power in zones with a temperate climate. A simplified model based on the energy balance in the solar collectors considering the main operating parameters of the typical solar power plant was developed. It should be noted here that the model does not take into account issues related to heat accumulation and electricity generation in a Solar Thermal Power Station. The simulation of forced convection inside the solar collector absorber was additionally included in the calculations to improve its accuracy. The model was verified using actual heat measurements at the outlet of the parabolic collector installation at a Solar Thermal Power Station located in the south of Spain. The heat generated by a similar solar collector system in a selected region with a temperate climate, the city of Bialystok (north-eastern Poland, geographic coordinates: 53°08′07″N 23°08′44″E) was determined by the developed simplified model for different months of the year. Based on the results of the analysis, it was found that the energy obtained from the same area of concentrated solar collectors located near Bialystok is eight times lower compared to the location in Cordoba depending on the variant of the power plant operation.

Keywords: concentrating solar power systems; solar gains; solar plants; parabolic trough collectors

1. Introduction

Solar energy is one of significantly developing branches of renewable energy sources. Total annual solar radiation on the surface of the Earth is estimated to be about 7500 times higher than the annual global consumption of primary energy [1]. Trends in new investments in solar systems sector show 23% increase, comparing to 2004, whereas a period between 2013 and 2018 was marked by both: annual falls and growths [2]. According to forecasts [3] the share of fuels in overall energy balance will continue changes and instead of two-thirds fossil fuels in 2018, two-thirds zero-carbon energy by 2050 will be reached, supplying almost 50% of world electricity from solar and wind energy, 50-by-50. On December 11, the Council of Europe approved a plan that will raise the CO2 reduction target from 40 percent to at least 55 percent by 2030 [4]. Thus far, concentrating technologies using parabolic trough collectors (PTC) were used in countries with high radiation and is responsible for more 96% of installed CSP power [5]. As reported by [6] PTC-based solar thermal systems are mostly used in electricity generation systems, accounting for approximately 85% of total current installed capacity worldwide.

Currently the most parabolic trough solar thermal power plants (PTSTPP) are in Spain and the USA [7]. In the literature, examples of models of such systems and analysis

of possible improvements were presented. Knysh [8] proposed a model of the flow dynamics and heat exchange in the tube receiver of a solar parabolic trough module (PTM) to be used during designing solar energy systems with PTC of different power. Tatebi et al. [9], using a numerical model and experimental data, investigated the effect of metal foams and nanofluids on the thermal performance of a direct absorption parabolic trough collector (DAPTC). Authors concluded that porous media with high absorption coefficient and scattering coefficient could absorb more incoming radiation and transfer to heat transfer fluid, thus the increase in the collector's efficiency can be obtained. Possibilities to improve the absorber tube of a parabolic trough collector, resulting in a heat transfer enhancement was proposed by Aldulaimi [10]. Abbas et al. [11,12] analyzed different locations in Spain and compared efficiency of PTCs and Linear Fresnel Collectors (LFCs). The results of the optimization by means of a validated Monte Carlo Ray Trace code and analytic methods showed higher annual efficiency in the case of PTCs. Hongn et al. [13] studied end optical losses of collectors. Salazal et al. [14] developed and valuated an analytic modelling of the energy flows in parabolic trough solar thermal power plants that allows for evaluation of energy savings in a case of potential modifications in components, system design and location. Whereas Ma at al. [15] presented a thermal hydraulic model solved by a novel numerical approach based on graph theory and the Newton–Raphson method. Rogada et al. [16] focused on a heat transfer fluid (HTF) used to transfer the thermal energy of solar radiation through parabolic collectors to a water vapour Rankine cycle, and proposed a model to optimize the temperature of the fluid. Similar problems were analysed by Barcia at al. [17] and a dynamic model of the HTF heating process was proposed. It included main fluid properties such as density, thermal conductivity or specific heat, thus the model was not limited to commonly used synthetic oil. On the other hand Llamas et al. [18–20] developed of a mathematical model for the optimal operation of parabolic-trough power plants with different power in context of their integration into electricity markets with minimizing grid-connection costs.

Recently, the solar market trend in developed countries seems to be stabilizing. In 2017, the solar investments in developing countries were much higher (USD 115.4 billion) than in developed economies (USD 45.4 billion) that comparing with 2016 is in line with 41% increase and 17% fall, respectively [2].

The vast majority of publications related to parabolic solar collectors concern a tropical or subtropical climate [21–24], which is understandable due to the significant DNI values in these regions. In the case of temperate climate, scientific publications focus mainly on flat plate collectors [25–28], which are most often used for domestic hot water heating. It should be emphasized here that parabolic solar collectors can generate high temperature of the medium in the absorber, which is why they are often used in thermal power plants. Flat solar collectors without a mirror system, which are used in temperate climates to heat domestic hot water, do not require such high temperature as parabolic solar collectors. No information has been found in the literature on the operation of parabolic solar collectors in the literature on the operation of parabolic solar collectors in temperate climates.

In the case of electricity production in temperate climates, photovoltaic (PV) panels are commonly used [29]. The main advantage of photovoltaic panels is the use of diffusive radiation to generate electricity [30]. In areas with high values of solar radiation (tropical climate), CPS power plants based on parabolic solar collectors generate about 33% [31] more electricity than PV power plants. Power plants based on photovoltaic cells and parabolic solar collectors can be combined into hybrid systems [32].

The computational methods used in simulations of the operation of parabolic solar collectors can be divided according to the complexity of the model geometry. In the most extensive three-dimensional numerical methods, thermal parameters on the absorber walls are determined depending on the mirror system or the absorber shape, as a result of which it is possible to design new constructions of focusing solar collectors [33–35]. Three-dimensional calculations are most often performed with the use of complex computational programs Ansys-Fluent [34] or OpenFOAM [35]. The second group of thermal-

flow calculations in solar collectors is related to the problem of the two-dimensional cross-section of the solar collector and it is most often a simplification of three-dimensional problems [36]. Both the two-dimensional and three-dimensional problems are determined using advanced computational fluid dynamics (CFD) programs with a heat exchange module. The third group are issues related to one-dimensional flow and they can be used to design solar collector installations with infrastructure. In the case of one-dimensional problems, specialized software, e.g., System Advisor Model (SAM) [22,24], TRNSYS [37] are also used. Sometimes custom source codes are created [21,38]. They require an appropriate programming environment, e.g., Matlab or the ability to write own computer programs [39]. The most popular program System Advisor Model (SAM) [40] can be used for the initial analysis of the entire solar power plant, where three areas can be distinguished: solar collector installations, heat storage tanks and devices for generating thermal energy (solar field, thermal storage, power block). All these modules in a thermal power plant are interconnected into one system. In the case of the analysis of individual devices that are part of a thermal power plant, it is good practice to use classic equations resulting from thermal-flow issues. Due to the lack of data on the operation of parabolic collectors in temperate climates, a simplified model of estimating heat generated by parabolic collectors has been developed, which can be implemented in a spreadsheet, e.g., MS Excel or Apache OpenOffice. The developed simplified algorithm for the operation of parabolic solar collectors was determined on the basis of the problem of forced convection in the absorber [41]. The presented model does not take into account the dynamics of the system and devices included in the thermal power plant [17]. Dynamic modeling [17] of solar power plants introduces possibilities of optimizing the operation of solar parabolic collectors.

In this paper, a simplified model to evaluate solar energy gains from PTSTPP in different locations was developed. Moreover, using this model it is possible to estimate an area of the parabolic through solar field (PTSF) necessary to deliver the energy to meet the assumed target. The validation of the developed model was performed by comparing its results with the heat generated by a set of parabolic solar collectors at a real thermal power plant in the south of Spain. The results of this type of simulations could be useful for preliminary analysis of the CSC systems applications. The presented model has been implemented in an MS Excel spreadsheet. The aim of the work is also to investigate the numerical work of parabolic solar collectors in a temperate climate based on the existing solar installation in Spain.

2. Simplified Model of Heat Production Forecasting by Concentrating Solar Collectors

Figure 1 shows the satellite view of a solar power plant. In this power plants (geographic coordinates: 37°45′18.00″ N 5°3′26.00″ W), five basic parts can be distinguished (Figure 2): from parabolic solar collectors with pipelines, heat storage tanks, a set of heat exchangers in which steam is produced, steam turbines with an alternator and devices for cooling the medium from the steam turbine. The description of the elements of the collector field and the main parameters of this Solar Plant are presented in Tables 1 and 2, respectively. The HTF parameters adopted in Table 2 were determined for the average temperature at the outlet and inlet of a single loop $(T_{in} + T_{out})/2$. The collector thermal efficiency η_{CPS} in Table 2 is defined as the ratio of the useful energy delivered to the energy incident on the collector aperture. Parabolic solar collectors are the most effective and most widely used method of large-scale heat generation. Parabolic collectors (Figure 3) are composed of mirrors that reflect and focus solar radiation on pipes (absorber) filled with HTF. The liquid is then transported to the steam generation system, then the steam is used in a steam turbine to generate electricity.

Figure 1. View of solar cylinder parabolic collectors at the Solar Thermal Power Plant "La Africana" ("satellite" view from googlemaps.com).
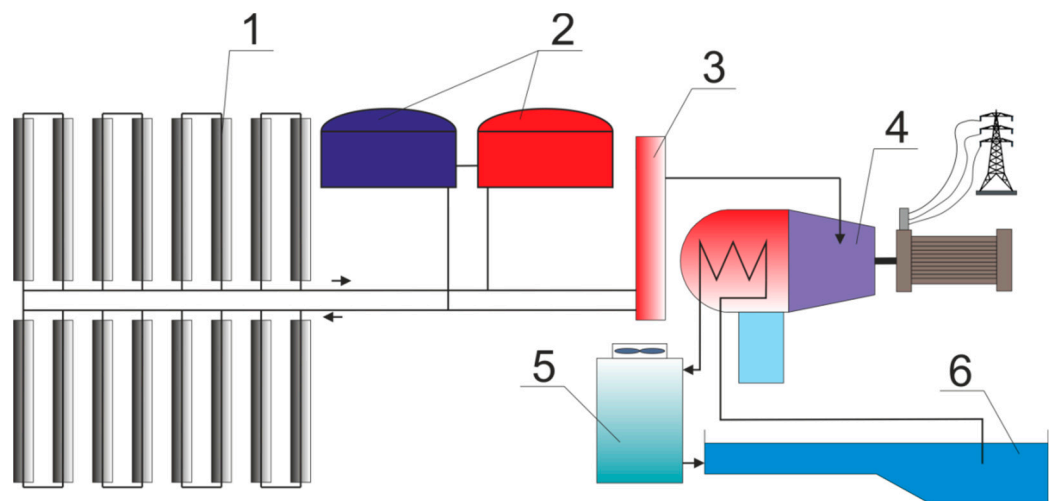

Figure 2. Simplified diagram of a thermal power plant with parabolic solar collectors: **1**—parabolic solar collectors, **2**—heat storage tanks, **3**—steam generation system, **4**—steam turbine, **5**—cooling tower, **6**—water storage reservoirs.

Table 1. Description of the elements of the collector field in the Solar Thermal Power Station of te south of Spain.

| Description	Value	Unit
Number of mirrors in a single solar collector:	28	-
Mirrors surface area in a single solar collector:	68.2	m²
Number of solar collectors:	8064	-
Surface area of all mirrors:	549,965	m²
Number of loops:	168	-
Number of solar collectors included in one loop:	48	-
Number of absorbers:	24,192	-
The length of a single loop:	556.00	m
Absorber diameter	0.07	m
Diameters of pipes transporting HTF	0.1143–0.61	m
Diameters of the outer coats of thermal insulation of pipelines transporting HTF	0.2–0.8	m
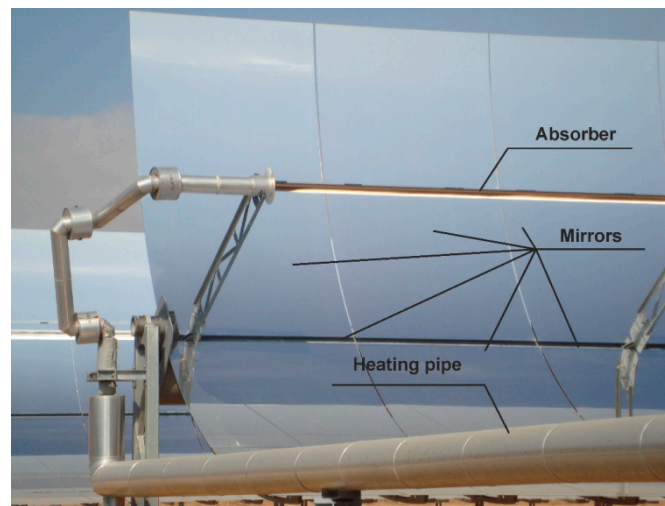
Figure 3. Detail of a cylindrical-parabolic solar collector of a Solar Thermal Power Station (photo by T.J. Teleszewski).

Table 2. Operation parameters of the Solar Thermal Power Station of the south of Spain.

Loop Inlet Temperature	T_{in}	292	°C
Loop outlet temperature	T_{out}	392	°C
Mass flow through the absorber	m	7.06	kg/s
The dynamic viscosity of the HTF in the solar installation	μ	0.00017	kg/m/s
Thermal conductivity of the HTF in the solar installation	λ_m	0.0871	W/m/K
HTF density in the solar installation	ρ	757.85	kg/m³
Specific heat capacity of the HTF	c_p	2486.5	J/kg/°C
External convective heat transfer coefficient from the outside of the pipe	h_a	25	W/m²/K
Thermal conductivity of solar thermal insulation	λ	0.0871	W/m/K
Collectors thermal efficiency	η_{CPS}	0.47	-

The model focuses on the generation of heat by the collectors which is the part that depends strictly on the local climatic conditions. The location has a minimal impact on the operation and performance of the accumulation tanks and the power generators.

The hourly heat supplied by the solar collector system is determined from the following energy balance:

$$q_{num} = q_{CPS} - q_R - q_P \quad \text{(kWh)}, \tag{1}$$

where q_{CPS} is the heat obtained from all solar collectors in one hour, q_R is the heat losses at the receiver (absorber), and q_p is heat losses at heating pipes.

The heat obtained from the entire solar collector installation without heat losses is given by:

$$q_{CPS} = n_{loop} \cdot q_{loop} \quad \text{(kWh)}, \tag{2}$$

with n_{loop}, the number of loops, and $q_{loop}(t)$ is the hourly heat produced by a single loop.

The heat produced by a loop of collectors is:

$$q_{loop} = \pi \cdot D_a \cdot L_{loop} \cdot q_w \quad \text{(kWh)}, \tag{3}$$

where L_{loop} is the length of the absorber in a single loop, D_a is the diameter of the absorber, and q_w is the heat flux per 1 m² of the absorber, that can be calculated by:

$$q_w = \frac{DNI \cdot A_m \cdot K \cdot \eta_{endloss} \cdot \eta_{shadow} \cdot \eta_{opt} \cdot C_l}{\pi \cdot D_a \cdot L_{SOL}} \quad (\text{kWh/m}^2), \tag{4}$$

where L_{SOL} is the absorber length in a single solar collector, A_m is the mirror surface area, DNI is the direct normal irradiation, $\eta_{endloss}$ is the coefficient for the calculation of the relative end loss, η_{shadow} is the coefficient for solar shading, η_{opt} is the optical collector efficiency for perpendicular sun on collector which is assumed to be 0.75% based on research from the work [42], C_l is the mean cleanliness factor, while K is the Incident Angle Modifier.

The Incident Angle Modifier was determined according to the following equation [43]:

$$K = \cos(\theta_i) - 0.000525 \cdot \theta_i - 0.0000286 \cdot \theta_i^2 \tag{5}$$

where θ_i is the angle of incidence on the collector, with continuous east–west tracking, which was determined by the equation [44–47]:

$$\theta_i = \arccos\sqrt{\cos^2(\alpha) + \cos^2(\delta_s) \cdot \sin^2(\omega)} \tag{6}$$

$$\alpha = \arcsin[\sin(\delta_s)\sin(\phi) + \cos(\phi)\cos(\delta_s)\cos(\omega)] \tag{7}$$

$$\alpha_s = sign(\omega)\left| \arccos\left[\frac{\cos(90-\alpha) \cdot \sin\phi - \sin(\delta_s)}{\sin(90-\alpha)\cos\phi}\right]\right| \tag{8}$$

$$\delta_s = 23.45\sin(280.11 + 0.984d) \tag{9}$$

$$\omega = (t_{sol} - 12) \cdot 15° \tag{10}$$

where α is solar altitude angle, α_s is the solar azimuth angle, δ_s is the declination angle, ω is the hourly angle, t_{sol} is the solar time angle, ϕ is the latitude, and d is the number of the day of the year (from 1 for January 1 to 365 for December 31).

Coefficient for the end loss is determined according to the equation [48]:

$$\eta_{endloss} = 1 - \frac{L_f \tan(\theta_i)}{L_{PTC}} \tag{11}$$

where L_f is the focal length of the parabolic trough collector; L_{PTC} is the length of the parabolic trough collector.

The solar shading coefficient of the shadow from row to row at low solar altitude is given by the equation [44]:

$$\eta_{shadow} = |\cos(\rho_i)|\frac{L_s}{w} \tag{12}$$

where L_s is the distance from the center of the two PTCs, w is the aperture width, and ρ is the sun tracking angle described by the following relationship:

$$\rho = \tan^{-1}\left[\frac{\cos(\alpha_s)}{\tan(\alpha)}\right] \tag{13}$$

The basic condition for the correct operation of a single loop is to obtain the minimum temperature of HTF, T_{out}, at the outlet of a single loop for a nominal mass flow m:

$$T_{out} = \frac{q_{loop}}{m \cdot c_p} + T_{in}, \tag{14}$$

where T_{in} is the inlet temperature of the HTF at the entrance to the loop.

If the minimum temperature T_{out} is not achieved, in the presented simplified model it was assumed that the q_{loop} is equal to zero. Obtaining the set temperature at the outlet from the loop is a necessary condition for the correct operation of the solar power plant.

In the case of the analyzed solar power plant, the T_{out} temperature is in the range of 360 °C–392 °C. An increase in DNI causes an increase in the temperature of the medium in the absorber. As the temperature of the oil at the outlet of the absorber increases, the mass flow through a single loop increases (Figure 4a,b). When the maximum temperature at the outlet from the loop T_{out} = 392 °C is reached, the mass flow reaches the nominal value of 7.06 kg/s. In the event of a decrease in the T_{out} temperature in the evening hours (which is associated with a decrease in DNI), the mass flow decreases to the minimum value m = 0.01 kg/s. For practical reasons, it was assumed that q_{loop} is equal to zero if the required temperature T_{out} = 360 °C was not achieved.
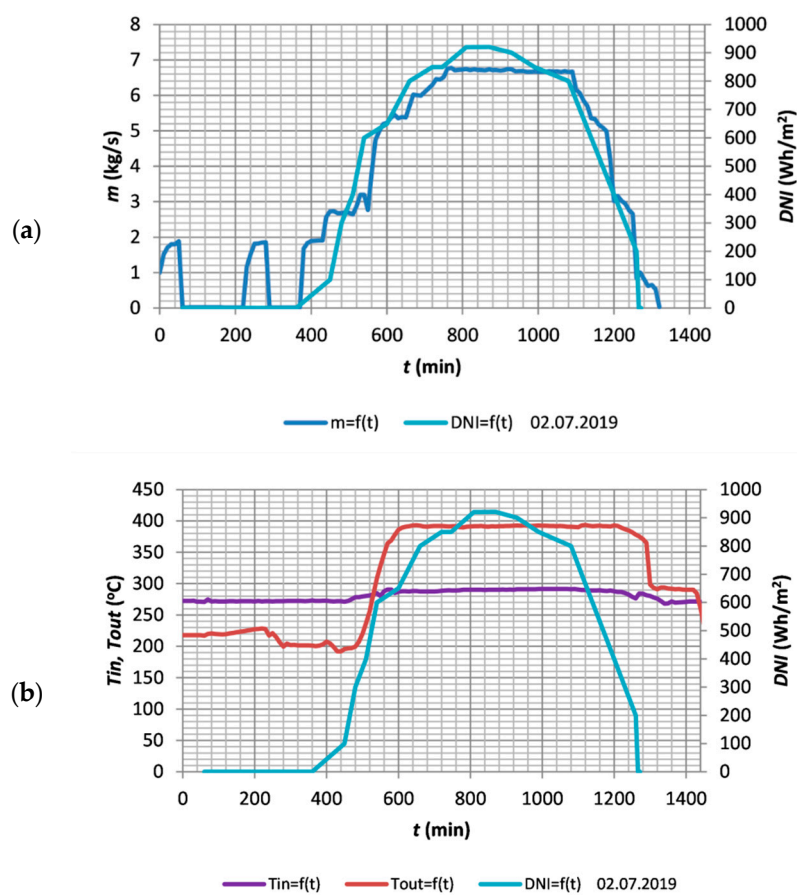
(**a**)

(**b**)

Figure 4. Changes in mass flow m (**a**) and temperature T_{in} and T_{out} (**b**) in a single loop on 02/07/2019 for the Solar Thermal Power Station in Spain.

The heat losses of pipelines are determined by the following equation:

$$q_P = \sum_{i=1}^{N} L_i \cdot q_i \ \ \text{(kWh)}, \tag{15}$$

where L_i is the length of pipe i and $q_i(t)$ is the heat losses per unit length of this pipe, that is given by:

$$q_i = \frac{(T_m - T_a)\pi}{\left(\dfrac{1}{2\lambda}\ln\left(\dfrac{D_i}{d_i}\right) + \dfrac{1}{h_a D_i}\right)1000} \ \ \text{(kW/m)}, \tag{16}$$

with T_m, the medium temperature, T_a, the average-hour outside temperature, d_i, the diameters of the pipes, D_i, the diameters of the thermal insulation around the pipelines, λ, the thermal conductivity of the thermal insulation, and h_a, the of the external convective heat transfer coefficient from the outside of the pipe.

The heat losses in the absorber were estimated based on the SCHOTT PTR®70 Receiver documentation available on the website of the absorber manufacturer [49]. To determine heat losses in the absorber, a heat loss curve was used [49] and the loops were divided into 50 elements. Calculations of heat losses in the absorber were made for the current oil temperature. Assuming a constant heat flux along the absorber walls, a linear increase in the average temperature of the medium flowing in the absorber was obtained:

$$T_m(x) = T_{in} + \frac{q_w \cdot \pi \cdot D_a}{m \cdot c_p} x \ \ (°C),$$ (17)

where $T_m(x)$ is the temperature which varies with length x of the absorber.

3. Validation of the Presented Model Through Heat Measurements in an Existing Solar Thermal Power Station in Spain

The validation of the presented simplified model for estimating heat production by parabolic solar collectors was performed by comparing the heat determined from the Equation (1) with the heat measured in the parabolic solar collectors at a thermoelectric solar plant in the south of Spain (Solar Thermal Power Plant "La Africana", Tables 1 and 2) three selected day from 2019 with different climate conditions: 07/02/2019, 03/22/2019, and 09/09/2019.

The actual values of direct solar radiation measured in Cordoba were used for the calculations. In the Solar Thermal Power Station of the south of Spain, the automation of parabolic solar collectors is equipped with east–west tracking and is characterized by high percentage tracking performance. Percentage tracking performance [50] is a parameter that compares the absorbed energy for a given type of tracking in relation to the absorbed energy of full tracking according to the equation:

$$Percentage\ tracking\ performance = \frac{Absorbed\ energy\ for\ a\ given\ type\ of\ tracking}{Absorbed\ energy\ for\ full\ tracking} 100 \ \ (\%)$$ (18)

Figure 5 shows the percentage east–west tracking performance in southern Spain compared to full tracking mode for the four selected days. East–west tracking is relatively similar compared to full tracking.
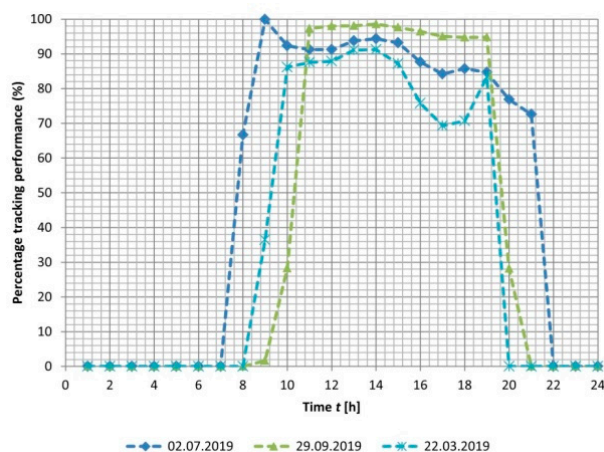
Figure 5. Percentage tracking performance compared to full tracking mode on selected days at the Solar Thermal Power Station in Spain.

The calculations assumed the mass flow in the range from 5 kg/s to 7.06 kg/s with the minimum temperature condition (Equation (14)) at the outflow from the loop equal to 360 °C. In fact the flow increases gradually with the increase in direct solar radiation, reaches its maximum value equal to 7.06 kg/s and then decreases in the evening with the decrease in solar radiation. An example of the course of changes in the mass flow measured on 02/07/2018 in a single loop is shown in Figure 4a,b. It should be noted here that in practice, solar collectors

are used to produce heat for a solar power plant only when the required temperature at the outlet from the solar system is achieved and at nominal mass flow.

With these assumptions, the heat flux per square meter of the absorber can be calculated by Equation (4). Figure 6 shows calculations of this heat flux density together with DNI for selected days in the Spanish Solar Plant. The maximum unit heat flux is about 25 kW per square meter of the absorber.
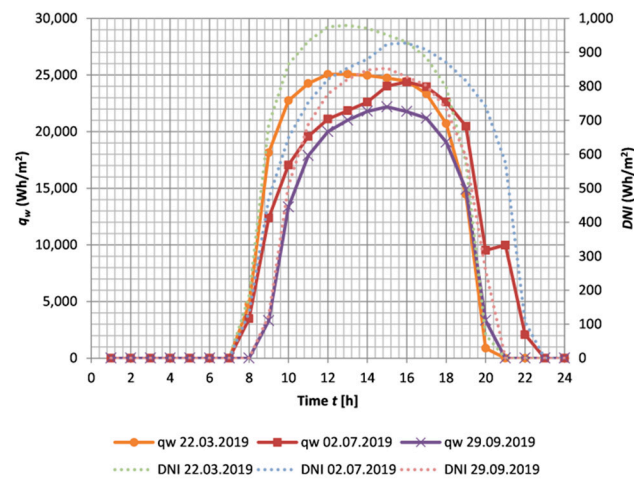

Figure 6. Calculated heat flux density per one square meter of an absorber and DNI for selected days for the Solar Thermal Power Station in Spain.

The next stage of model validation consisted in comparing the numerical values of annual heat q supplied by the solar collector system, calculated by Equation (1), and actual values measured in Solar Plant for selected days of the year: 22/03/2019, 02/07/2019 and 29/09/2019. The results of this comparison are shown in Figure 7a–c. A good agreement is found between the measured and calculated values of annual heat supplied by the collector field for the different dates. This agreement shows the goodness of the model. The observed differences between these values is caused by the control of the flow in the absorber by the automatic control system. The simulations in this work were performed for the flow in the range from 5 kg/s to 7.06 kg/s.
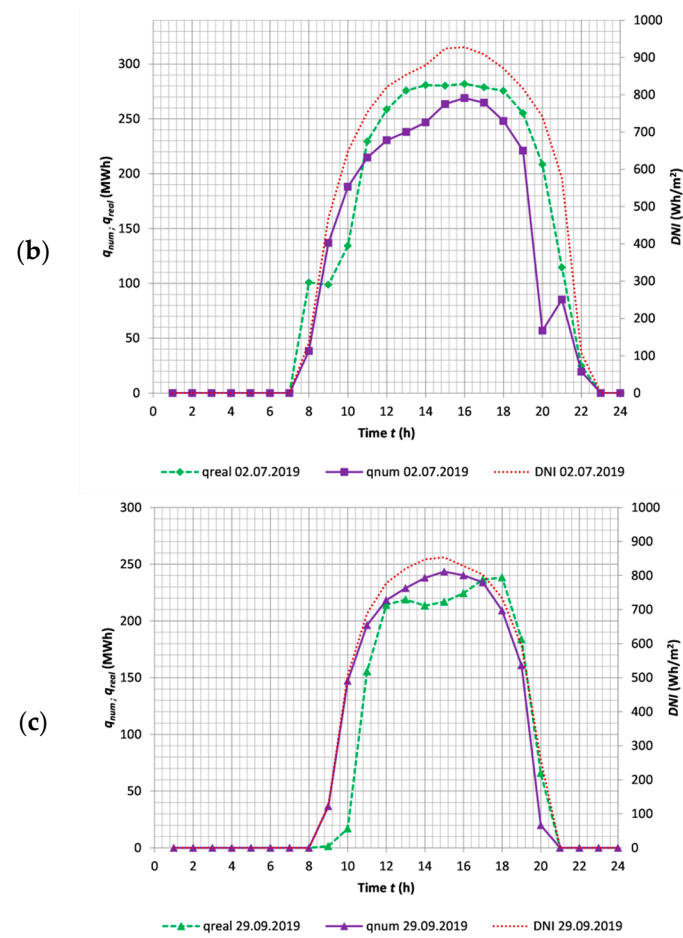

(**a**)
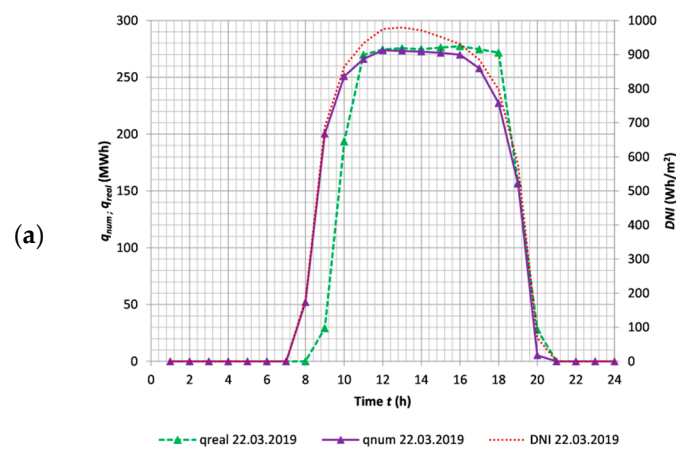
Figure 7. Comparison of heat produced by solar collectors with heat determined from the developed model the Solar Thermal Power Station in Spain for selected days: (**a**) 22.03.2019, (**b**) 02.07.2019, (**c**) 29.09.2019.

According this comparison, the relative error of the developed model was determined according to the following relationship:

$$\delta q_{num} = \left| \frac{q_{real} - q_{num}}{q_{real}} \right| 100\% \,, \tag{19}$$

where q_{num} is the heat determined from Equation (1) and q_{real} is the heat measured in the thermoelectric solar plant in Spain, Cordoba province. Table 3 presents the calculation results of the model and the actual values of heat produced by parabolic solar collectors in March, July and September. The calculations also considered the shutdown time of parabolic solar collectors intended for conservation works and for March, July and September, respectively, 11, 3 and 4 days. The relative error of the presented model for the selected months did not exceed 7.1%.

Table 3. Relative Errors of the model in the selected days.

Selected Month	Number of Days in the Month When Solar Collectors Were Turned off	Heat Measured q_{real}	Heat Determined from the Model q_{num}	Relative Error δq_{num}
		MWh	MWh	%
March 2019	11	22,043	20,508	6.96
July 2019	3	61,076	64,210	−5.13
September 2019	4	43,312	40,249	7.07

Figure 8 shows the temperature dependence on the output of a single loop consisting of 48 solar collectors as a function of the density of DNI and mass flow in the absorber. With the decrease in mass flow in the absorber and the increase in solar radiation intensity, the temperature at the outlet from a single loop increases. The minimum temperature at the outlet of a single loop is 360 °C and is achieved for DNI of 450 Wh/m², 670 Wh/m² and 905 Wh/m² for flow rates of 5 kg/s, 7 kg/s and 10 kg/s, respectively. In the case of a working temperature of 392 °C, it is obtained for 680 Wh/m², 920 Wh/m² for 5 kg/s and 7 kg/s, respectively. With a mass flow of 10 kg/s, the operating temperature is not reached for the maximum DNI. The maximum operating temperature of 400 °C is achieved with a flow of 5 kg/s.
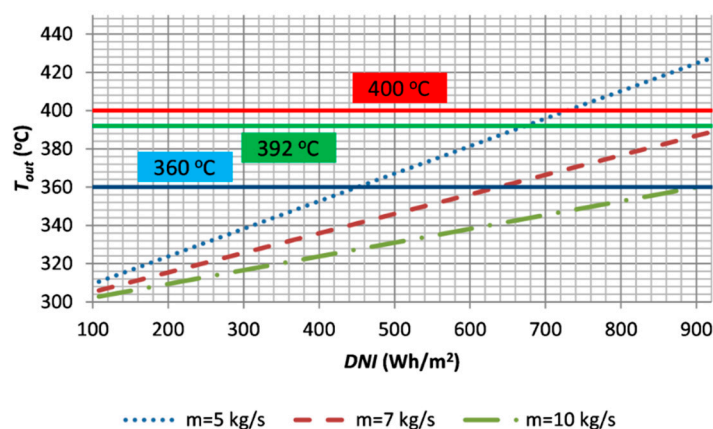

Figure 8. Medium temperature in the absorber at the outlet of a single loop as a function of mass flow and solar radiation (calculations performed for the conditions in Cordoba).

Figure 9 shows an example of the temperature distribution of the medium flowing through the absorber as a function of the absorber length for a single loop for a constant mass flow of 6 kg/s and selected DNI: 1000 W/m², 800 W/m², 600 W/m² and 400 W/m². The calculations were made according to the equation (8). The resulting linear rise in temperature of the medium in the absorber is typical of the constant condition of the heat flux along the walls [41] of the absorber.
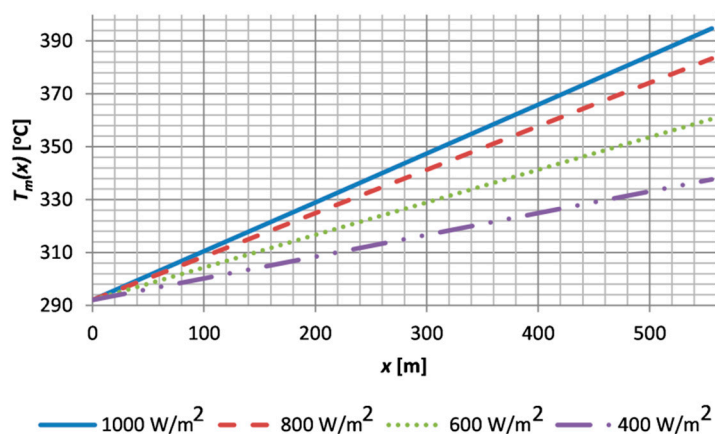

Figure 9. Temperature distribution of the medium flowing through the absorber as a function of the absorber length for different DNI.

The results of calculations of the convective heat transfer coefficient inside the absorber are presented below. For this purpose, a simplified model of forced convection for

turbulent flow was used. The local convective heat transfer coefficient is described by the following equation:

$$h_f = \frac{\mathrm{Nu}_D \lambda}{D},$$ (20)

where D is the absorber diameter, λ is the conductivity coefficient of the medium, while the Nusselt number is described by the Dittus–Boelter correlation:

$$Nu_D = 0.023\,\mathrm{Re}^{4/5}\,\mathrm{Pr}^{0.4}, \quad \mathrm{Re} \geq 10000, \quad 0.6 \leq \mathrm{Pr} \leq 1600, \quad \mathrm{Pr} = \frac{c_p \mu}{\lambda}, \quad \mathrm{Re} = \frac{4m}{\pi D \mu},$$ (21)

where Re is the Reynolds number, while Pr is the Prandtl number.

Figure 10 shows the relationship of convective heat transfer coefficient. The convection coefficient increases with increasing flow through the absorber. With a nominal flow value of $m = 7.06$ kg/s, the convective heat transfer coefficient is 2714 W/(m²K). The determined value of the convective heat transfer coefficient is relatively high compared to the values determined in the literature [33,38], which is the result of much larger real Reynolds numbers in relation to the Reynolds numbers from works [33,38]. Increasing the mass flow of the medium in the absorber to 10 kg/s increases the convective heat transfer coefficient by about 24%.
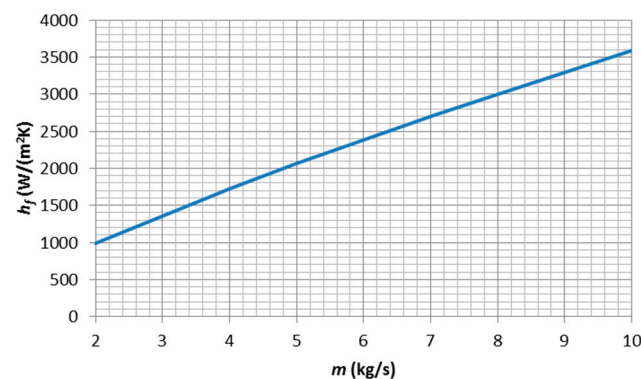

Figure 10. Convective heat transfer coefficient as a function of mass flow in the absorber.

4. Application of the Model for the Performance Prediction of a Solar Thermal Power Station Located in a Temperate Climate Location

This chapter presents the results of calculations of heat produced by a system of parabolic solar collectors for a selected region of temperate climate: in the city of Bialystok located in the north-eastern part of Poland. The climatic conditions of this localization are presented in Figure 11 and compared with Spanish conditions. The main differences with the south of Spain are much lower values of direct solar radiation and temperature, which is mainly due to the different latitude. The annual value of DNI in Cordoba was 1938 kWh/m²/year, while in the case of Bialystok, the annual DNI is 467 kWh/m²/year.

The correct operation of a thermoelectric power plant depends on the minimum temperature at the outlet of the solar installation, giving by Equation (14), which is 360 °C for a thermoelectric power plant in Spain in the Cordoba province, therefore two variants were adopted for the calculations:

- Variant A, the result of the calculations is the heat produced by parabolic solar collectors without considering the minimum temperature at the outlet from a single loop of 48 solar collectors,
- Variant B, the result of the calculations is the heat produced by parabolic solar collectors, considering the minimum temperature at the outlet of a single loop of 48 solar collectors equal to 360 °C.

In the case of variant A (Figure 12a), the heat generated in the south of Spain by the presented parabolic collectors is approximately four times greater than in the case of Bialystok (Table 4) Parabolic collectors require direct radiation, which is also four times lower in Bialystok compared to South of Spain (Figure 11a). Diffuse solar radiation (Figure 11b) in Spain and Bialystok is similar but, unfortunately, it does not play a significant role in the production of heat in the case of concentrating solar collectors.

Table 4. Annual heat produced by solar collectors in Spain (Cordoba) and Poland (Bialystok).

Region	Case A	Case B
	Heat (MWh)	
South of Spain	528,388	406,383
Poland (Bialystok)	132,536	52,269

In the case of variant B (Figure 12b), the estimated amount of heat generated by solar collectors in Bialystok is eight times lower than the amount of heat produced by solar collectors in the south of Spain (Table 4). The greatest differences between the heat produced in Spain and Bialystok are in the fall and winter months, and the smallest in the summer. As in variant A, these differences are mainly caused by a small share of direct solar radiation and low outdoor temperature in Poland compared to southern Spain (Figure 11c). Higher temperature of the medium in the absorber and lower temperature outside causes greater heat losses in the absorber and the solar pipes. In December, the expected heat production by parabolic solar collectors in Bialystok is close to zero for variant B.

Many publications [18–20,51–54] describe studies of the use of parabolic collectors for thermoelectric power plants in countries such as Greece, Spain, China and Nigeria, which are located in the subtropical and tropical climatic zone, i.e., in the area where direct solar radiation is significant. The territory of Poland is located in a temperate climate zone, which is not recommended by producers of parabolic solar collectors used to produce heat for the operation of typical steam turbines.
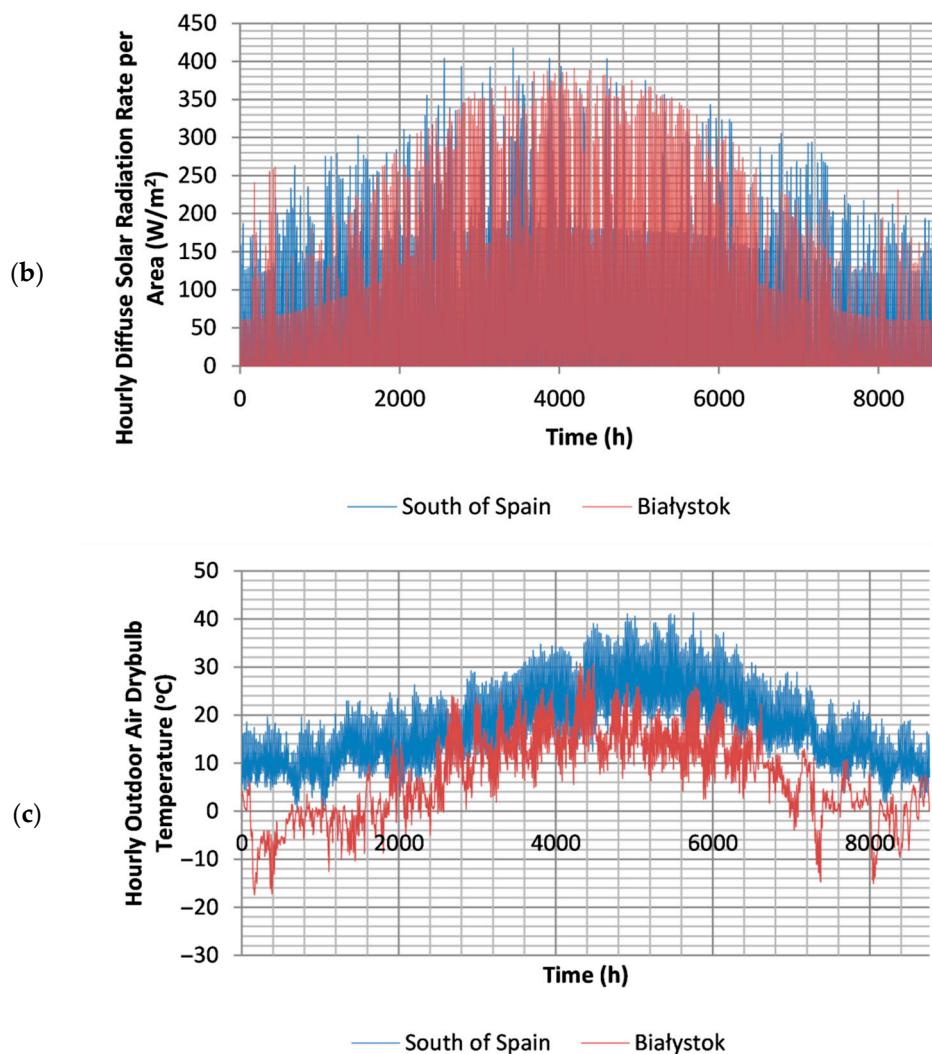
(a)
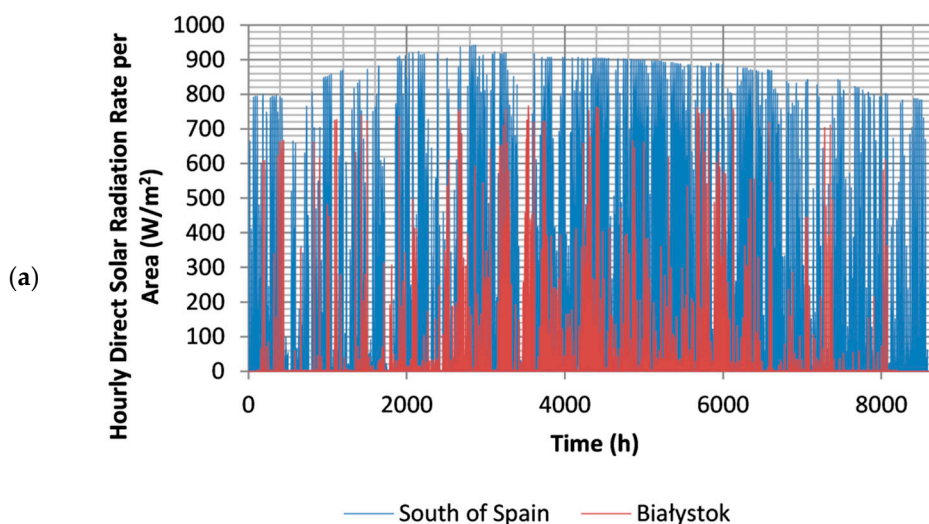
Figure 11. Hourly annual distribution of direct solar radiation (**a**), diffuse solar radiation (**b**) and outdoor temperature (**c**).

According to the SCHOTT PTR®70 Receiver brochure [49], the worldwide uses are divided into four categories: "Excellent", "Good", "Satisfactory", "Unsuitable". The map of the use of solar collectors [49] is consistent with the map of annual solar radiation in the world [55]. Cordoba is in the area marked "Good", while Bialystok is labelled "Unsuitable". The above calculation results using the simplified model confirm this fact. Comparing the map in SCHOTT PTR®70 Receiver [49] with the map of the distribution of climatic zones [53], it can be noticed that the best location of parabolic solar collectors is the climate of the tropical and subtropical zones, excluding parts of South America and Africa with tropical rainforest.

One solution to increase the heat production of parabolic solar collectors in temperate climates is to use more collectors in a single loop, which allows for higher heat production with a lower DNI value. The disadvantages of this solution are additional investment costs, higher hydraulic losses in the loops and significant fluctuations in the medium flow in the absorber.

It should be noted that the simplified algorithm based on the forced convection presented in this paper may be useful for estimating the heat production by solar collectors in a solar thermal power station under various climatic conditions.
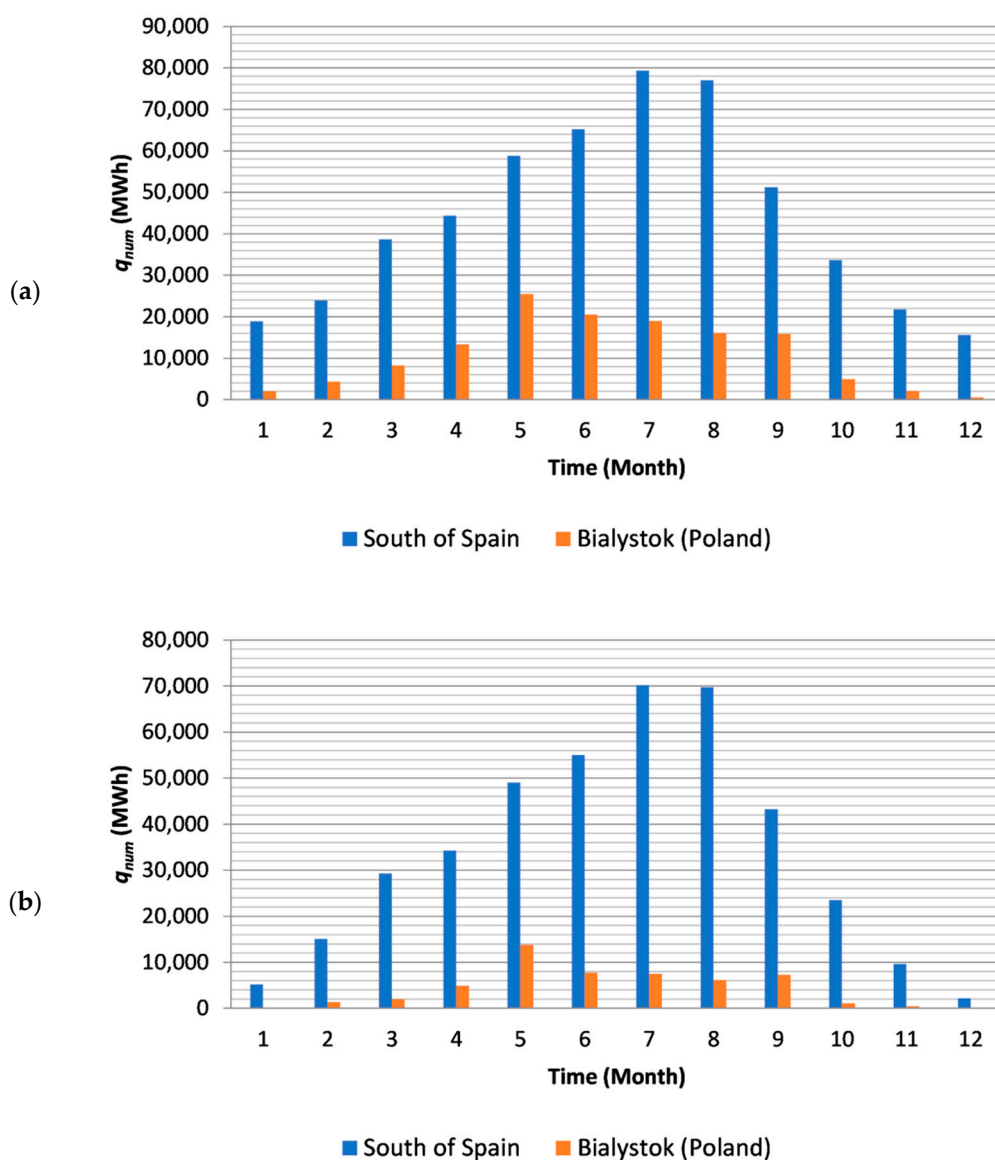
(**a**)

(**b**)

Figure 12. Annual heat produced by parabolic solar collectors for variants A (**a**) and B (**b**).

5. Conclusions

A simplified model for evaluation of solar energy gains from PTSTPP was developed and verified on based on data measurements data. The relative error of the presented algorithm based on the forced convection for the selected months did not exceed 7.1%, thus it should be noted that the model can be used to estimate the heat production by parabolic solar collectors, considering metrological conditions and temperature at the outlet from the solar installation for different climatic zones. The simplified method of estimating heat production by parabolic solar collectors presented in this paper may be an alternative to the most commonly used computer programs, such as SAM, in which simulations are performed for ready-made diagrams of thermal power plants. The presented method makes it possible to estimate the heat generated by parabolic solar collectors, regardless of the typical schemes of a thermal power plant with a part of heat accumulation in storage tanks and a part related to the production of electricity. The main advantage of the presented method is the possibility of quick implementation of the presented equations in spreadsheets.

Thermoelectric plants equipped with parabolic solar collectors are dynamically developed as alternative energy sources in the area of tropical and subtropical climate. The results of calculations using a simplified calculation model, which were verified on the

existing thermoelectric plant, indicate that the thermal efficiency of parabolic solar collectors working with standard steam turbines is eight times lower than in the case of the existing thermoelectric plant in the south of Spain. Therefore, it can be concluded that in the climatic conditions of Poland, the use of solar plant based on concentrated solar collectors is not justified. In the opinion of the authors the solution to the problem is the use of low-temperature technologies, which will be the subject of further research on the viability of using Parabolic Trough Solar Thermal Power Plants in moderate climate conditions.

Nomenclature

A_m	mirror surface area(m^2)
C_l	mean cleanliness factor
c_P	specific heat capacity of the HTF (J/kg/°C)
d	number of the day of the year (from 1 for January 1 to 365 for December 31)
d_i	diameters of the pipes (m)
D_a	absorber diameter (m)
D_i	diameters of the thermal insulation of the pipelines (m)
DNI	direct normal irradiance for hourly values (Wh/m^2)
h_a	external convective heat transfer coefficient from the outside of the pipe ($W/m^2/K$)
h_f	local convective heat transfer coefficient ($W/m^2/K$)
K	Incident Angle Modifier (-)
L_f	focal length of the parabolic trough collector (m)
L_{loop}	absorber length in a single loop (m)
L_{PTC}	length of the parabolic trough collector (m)
L_S	distance from the center of the two PTCs (m)
m	mass flow rate through the absorber (kg/s)
n_{loop}	number of loops (-)
Nu_D	Nusselt number (-)
Pr	Prandtl number (-)
q_{CPS}	heat obtained from all solar collectors during one hour (kWh)
q_{loop}	hourly heat produced by a single loop (kWh)

q_{num}	hourly heat supplied by the solar collector system (kWh)
q_P	heat losses from heating pipes (kWh)
q_R	heat loss from the absorber (kWh)
Re	Reynolds number (-)
t_{sol}	solar time angle (h)
T_a	average-hour outside temperature (°C)
T_{in}	single loop inlet fluid temperature (°C)
T_m	medium temperature (°C)
T_{out}	single loop outlet fluid temperature (°C)

Greek symbols

α	solar altitude angle (degree)
α_s	solar azimuth angle (degree)
δ_s	declination angle (degree)
$\eta_{endloss}$	coefficient for the calculation of the relative end loss (-)
η_{opt}	optical collector efficiency for perpendicular sun position (-)
η_{shadow}	coefficient for solar shading (-)
θ_i	angle of incidence on the collector surface (degree)
λ	thermal conductivity of the thermal insulation (W/m/K)
λ_m	thermal conductivity of the medium (W/m/K)
μ	dynamic viscosity of the HTF in the solar installation (kg/m/s)
ρ	sun tracking angle (degree)
ϕ	Latitude (degree)
ω	hourly angle (degree)

Abbreviations

CSC	Concentrated Solar Collector
HTF	Heat Transfer Fluid
PTC	Parabolic Trough Collector
PTR	Parabolic trough reflector
PTSTPP	Parabolic trough solar thermal power plant
PTSF	Parabolic trough solar field

References

1. Thirugnanasambandam, M.; Iniyan, S.; Goic, R. A review of solar thermal technologies. *Renew. Sustain Energy Rev.* **2010**, *14*, 312–322.
2. Available online: http://www.iberglobal.com/files/2018/renewable_trends.pdf (accessed on 11 March 2021).
3. Available online: https://bnef.turtl.co/story/neo2019 (accessed on 11 March 2021).
4. Available online: https://euobserver.com/green-deal/150364 (accessed on 11 March 2021).
5. Zhang, H.L.; Baeyens, J.; Degrève, J.; Cacères, G. Concentrated solar power plants: Review and design methodology. *Renew. Sustain. Energy Rev.* **2013**, *22*, 466–481.
6. International Renewable Energy Agency. Renewable Power Generation Costs in 2014. Available online: https://www.irena.org/-/media/Files/IRENA/Agency/Publication/2015/IRENA_RE_Power_Costs_2014_report.pdf (accessed on 1 March 2021).
7. Rodero, A.; Krawczyk, D.A. Development of renewable energy. In *Bulidings 2020+.Energy Sources*; Krawczyk, D.A., Ed.; Printing House of Bialystok Univesity of Technology: Bialystok—Cordoba—Vilnius (Poland-Spain-Lithuania), 2019; doi:10.24427/978-83-65596-73-4_1.
8. Knysh, L. Modeling of the Turbulent Heat and Mass Transfer in the Receiver Systems of the Solar Parabolic Trough Modules. *Appl. Sol. Energy* **2018**, *54*, 444–447.
9. Tayebi, R.; Akbarzadeh, S.; Valipour, M.S. Numerical investigation of efficiency enhancement in a direct absorption parabolic trough collector occupied by a porous medium and saturated by a nanofluid. *Environ. Prog. Sustain. Energy* **2018**, *38*, 2, 727–740.
10. Al Dulaimi, R.K.M. An Innovative Receiver Design for a Parabolic Trough Solar Collector Using Overlapped and Reverse Flow: An Experimental Study Arabian Journal for Science and Engineering. *Mech Eng* **2019**, *44*, 7529–7539, doi:10.1007/s13369-019-03832-8.
11. Abbas, R.; Montes, M.I.; Rovira, A.; Martínez-Val, J.M. Design of an innovative linear Fresnel collector by means of optical performance optimization: A comparison with parabolic trough collectors for different latitudes. *Sol. Energy* **2017**, *153*, 459–470.
12. Abbas, R.; Montes, M.I.; Rovira, A.; Martínez-Val, J.M. Parabolic trough collector or linear Fresnel collector? A comparison of optical features including thermal quality based on commercial solutions. *Sol. Energy* **2016**, *124*, 198–215.
13. Hongn, M.; Larsen, S.F.; Gea, M.; Altamirano, M. Least square based method for the estimation of the optical end loss of linear Fresnel concentrators. *Sol. Energy* **2015**, *111*, 264–276.
14. Salazar, G.A.; Fraidenraich, N.; Alves de Oliveira, C.A.; Hongn, M. Analytic modeling of parabolic trough solar thermal power plants. *Energy* **2017**, *138*, 1148–1156.
15. Ma, L.; Wang, Z.; Lei, D. Establishment, validation, and application of a 3 comprehensive thermal hydraulic model for a 4 parabolic trough solar field. *Energies* **2019**, *12*, 3161, doi:10.3390/en12163161.
16. Rogada, J.R.; Barcia, L.A.; Martinez, J.A.; Menendez, M.; de Cos Juez, F.J. Comparative Modeling of a Parabolic Trough Collectors Solar Power Plant with MARS Models. *Energies* **2018**, *11*, 1–15, doi:10.3390/en11010037.
17. Barcia, L.A.; Peón Menéndez, R.; Martínez Esteban, J.Á.; José Prieto, M.A.; Martín Ramos, J.A.; de Cos Juez, F.J.; Nevado Reviriego, A. Dynamic Modeling of the Solar Field in Parabolic Trough Solar Power Plants. *Energies* **2015**, *8*, 13361–13377.
18. Llamas, J.M.; Bullejos, D.; Ruiz de Adana, M. Optimization of 100 MWe Parabolic-Trough Solar-Thermal Power Plants Under Regulated and Deregulated Electricity Market Conditions. *Energies* **2019**, *12*, 3973, doi:10.3390/en12203973.
19. Llamas, J.M.; Bullejos, D.; Ruiz de Adana, M. Optimal Operation Strategies into Deregulated Markets for 50 MWe Parabolic Trough Solar Thermal Power Plants with Thermal Storage. *Energies* **2019**, *12*, 935, doi:10.3390/en12050935.
20. Llamas, J.M.; Bullejos, D.; Ruiz de Adana, M. Techno-Economic Assessment of Heat Transfer Fluid Buffering for Thermal Energy Storage in the Solar Field of Parabolic Trough Solar Thermal Power Plants. *Energies* **2017**, *10*, 1123, doi:10.3390/en10081123.
21. Allouhi, A.; Benzakour Amine, M.; Kousksou, T.; Jamil, A. Yearly performance of low-enthalpy parabolic trough collectors in MENA region according to different sun-tracking strategies. *Appl. Therm. Eng.* **2018**, *128*, 1404–1419.
22. XU, X.; Vignarooban, K.; Xu, B.; Hsu, K.; Kannan, A.M. Prospects and problems of concentrating solar power technologies for power generation in the desert regions. *Renew. Sustain. Energy Rev.* **2016**, *53*, 1106–1131.
23. Mufti, G.M.; Jamil, M.; Naeem, D.; Mukhtiar, M.U.; Al-Awami, A.T. Performance Analysis of Parabolic Trough Collectors for Pakistan Using Mathematical and Computational Models. In Proceedings of the Clemson University Power Systems Conference (PSC), Clemson, CS, USA, 11–18 March 2016.
24. Bishoyi, D.; Sudhakar, K. Modeling and performance simulation of 100MW PTC based solar thermal power plant in Udaipur India. *Case Stud. Therm. Eng.* **2017**, *10*, 216–226.
25. Krawczyk, D.A.; Rodero, A.; Kolendo, Ł. Analysis of solar collectors' use in a single family house in Poland and Spain—A case study. In *IOP Conference Series: Earth and Environmental Science*; IOP Publishing: Bristol, UK, 2019; Volume 214, pp. 1–17.
26. Krawczyk, D.A.; Żukowski, M.; Rodero, A. Efficiency of a solar collector system for the public building depending on its location. *Environ. Sci. Pollut. Res.* **2019**, 1–10, doi:10.1007/s11356-019-05077-2.
27. Żukowski, M.; Radzajewska, P. A New Method to Determine the Annual Energy Output of Liquid-Based Solar Collectors. *Energies* **2019**, *12*, 1–12.
28. Badescu, V. Optimum size and structure for solar energy collection systems. *Energy* **2006**, *31*, 1819–1835.
29. Zdyb, A.; Gulkowski, S. Performance Assessment of Four Different Photovoltaic Technologies in Poland. *Energies* **2020**, *13*, 196, doi:10.3390/en13010196.
30. Adrada Guerra, T.; Amador Guerra, J.; Orfao Tabernero, B.; De la Cruz García, G. Comparative Energy Performance Analysis of Six Primary Photovoltaic Technologies in Madrid (Spain). *Energies* **2017**, *10*, 772, doi:10.3390/en10060772.

31. Awan, A.B.; Zubair, M.; Praveen, R.P.; Bhatti, A.R. Design and comparative analysis of photovoltaic and parabolic trough based CSP plants. *Sol. Energy* **2019**, *183*, 551–565, doi:10.1016/j.solener.2019.03.037.

32. Shaha, R.; Srinivasana, P. Hybrid Photovoltaic and Solar Thermal Systems (PVT): Performance Simulation and Experimental Validation. *Mater. Today: Proc.* **2018**, *5*, 22998–23006, doi:10.1016/j.matpr.2018.11.028.

33. Tzivanidis, C.; Bellos, E.; Korres, D.; Antonopoulos, K.; Mitsopoulos, G. Thermal and optical efficiency investigation of a parabolic trough collector. *Case Stud. Therm. Eng.* **2015**, *6*, 225–236, doi:10.1016/j.csite.2015.10.005.

34. Mathew, S.; Visavale, G.; Mali, V. CFD Analysis of a Heat Collector Element in a Solar Parabolic Trough Collector. In Proceedings of the International Conference on Applications of Renewable and Sustainable Energy for Industry and Society, Hyderabad, India, 27–29 October 2010; pp. 1–21, doi:10.13140/2.1.3247.4241.

35. Abed, N.; Afgan, I.; Cioncolini, A.; Iacovides, H.; Nasser, A. Assessment and Evaluation of the Thermal Performance of Various Working Fluids in Parabolic Trough Collectors of Solar Thermal Power Plants under Non-Uniform Heat Flux Distribution Conditions. *Energies* **2020**, *13*, 3776, doi:10.3390/en13153776.

36. Hachicha, A.; Rodriguez, I.; Lehmkuhl, O.; Oliva, A. On the CFD&HT of the Flow around a Parabolic Trough Solar Collector under Real Working Conditions. *Energy Procedia* **2014**, *49*, 1379–1390, doi:10.1016/j.egypro.2014.03.147.

37. Figaj, R.; Żołądek, M. Operation and Performance Assessment of a Hybrid Solar Heating and Cooling System for Different Configurations and Climatic Conditions. *Energies* **2021**, *14*, 1142, doi:10.3390/en14041142.

38. Jamali, H. Analyses of absorber tube of parabolic trough solar collector (PTSC) based on convective heat transfer coefficient of fluid. *Int. Energy J.* **2016**, *16*, 73–86.

39. Bellos, E.; Tzivanidis, C. Concentrating Solar Collectors for a Trigeneration System—A Comparative Study. *Appl. Sci.* **2020**, *10*, 4492, doi:10.3390/app10134492.

40. NREL SAM Help System for Version 29 November 2020. Available online: https:// sam.nrel.gov/images/web_page_files/sam-help-2020-11-29r1.pdf (accessed on 25 February 2021).

41. Shah, R.K.; London, A.L. *Laminar Flow Forced Convection in Ducts, Advanced in Heat Transfer*; Academic Press: London, UK, 1978.

42. Riffelmann, K.J. *Comparison Between PTR70 and UVAC: Efficiency Tests, Thermal Loss Measurements and Raytracing Experiments (in German)*. In: BMU Status Seminar, Stuttgart, July 1, 2005. https://scholar.google.com/scholar_lookup?title=Comparison%20between%20PTR70%20and%20UVAC:%20efficiency%20tests,%20thermal%20loss%20measurements%20and%20Raytracing%20experiments&author=K.%20J.%20Riffelmann&publication_year=2005 (accessed on 11 March 2021)

43. Rohani, S.; Fluri, T.P.; Dinter, F.; Nitz, P. Modelling and simulation of parabolic trough plants based on real operating data. *Sol. Energy* **2017**, *158*, 845–860.

44. Wagner, M.J.; Gilman, P. *Technical Manual for the SAM Physical Trough Model*; Tech. Rep.; Sandia National Laboratories: Albuquerque, NM, USA, 2011.

45. Duffie, J.; Beckman, W. *Solar Engineering of Thermal Processes*; John Wiley and Sons: Hoboken, NJ, USA, 2006.

46. Plana, I.; Polo, M.R.; Urrutia, R. *Tecnologia Solar*; Mundi Prensa: Madrid, Spain, 2005.

47. Bourges, B. Improvement in solar declination computation. *Sol. Energy* **1985**, *35*, 367–369.

48. Pandey, C.K.; Katiyar, A.K. Anote on diffuse solar radiation on a tilted surface. *Energy* **2009**, *34*, 1764–1769.

49. Available online: https://pdf.directindustry.com/pdf/schott-glas/schott-ptr70-brochure/22716-557455-_3.html (accessed on 1 March 2021).

50. Pombe, J.K.; Djalo, H.; Tibi, B.; Ayang, A. Optical performances of a solar parabolic trough collector for various solar tracking modes under climatic conditions of Maroua. *Int. J. Innov. Sci. Res* **2017**, *29*, 137–148.

51. Wang, J.; Wang, J.; Bi, X.; Wang, X. Performance Simulation Comparison for Parabolic Trough Solar Collectors in China. *Int. J Photoenergy* **2016**, *2016*, 9260943, doi:10.1155/2016/9260943.

52. Al-Soud Mohammed, S.; Hrayshat Eyad, S. A 50 MW concentrating solar power plant for Jordan. *J. Clean. Prod.* **2009**, *17*, 625–635.

53. El Gharbi, N.; Derbal, H.; Bouaichaoui, S.; Said, N. A comparative study between parabolic trough collector and linear Fresnel reflector technologies. *Energy Proc.* **2011**, *6*, 565–572.

54. Boukelia, T.; Mecibah, M.S. Parabolic trough solar thermal power plant: Potential, and projects development in Algeria. *Renew. Sustain. Energy Rev.* **2013**, *21*, 288–297.

55. Available online: https://www.researchgate.net/publication/333746713_Climate_Change_-_A_review/figures?lo=1 (accessed on 1 April 2021).